ISSN 0280-5316
ISRN LUTFD2/TFRT--5784--SE

Modelling of an EGR System

Fredrik Olin

Department of Automatic Control
Lund University
January 2007

Department of Automatic Control
Lund Institute of Technology
Box 118
SE-221 00 Lund Sweden

Document name
MASTER THESIS

Date of issue
January 2007

Document Number
ISRNLUTFD2/TFRT--5784--SE

Author(s)
Fredrik Olin

Supervisor
Johan Bengtsson at Volvo Powertrain in Gothenburg
Per Tunestål at Combustion Engines in Lund

Sponsoring organization

Title and subtitle
Modelling of an EGR System (Modellering av ett EGR-system)

Abstract
Due to new emission legislations in Europe and in the USA truck manufacturers are facing new difficulties when it comes to meeting these demands. This new legislation will demand more accurate models for simulation and malfunction diagnosis. The NOx emissions, covered in these new laws, are intimately linked to combustion temperatures and these temperatures may be decreased by means of exhaust gas recirculation into the intake air, so called EGR.
This thesis deals with alternative EGR mass flow estimation models in a 13-litre Volvo diesel engine equipped with turbo and variable geometry turbine. Using a mean value model and moving average filtered temperature, EGR valve position and pressures as inputs this estimate however, never touches the current EGR mass flow estimation in mean and maximum relative errors. Validation is by stationary inputs but dynamic simulations are examined.

Keywords
EGR, mean value engine model, and poppet valve.

Classification system and/or index terms (if any)

Supplementary bibliographical information

ISSN and key title
0280-5316

ISBN

Language
English

Number of pages
40

Recipient's notes

Security classification

Acknowledgement

I would like to thank Volvo Powertrain and Johan Bengtsson for providing this master thesis assignment. Furthermore, I am grateful for the help provided by Per Tunestål and Rolf Johansson.

Fredrik Olin
Lund, December 2006

Notation

Signal names can be seen under measurements.

Variable/constant/abbreviation	Explanation	Unit
$\dot{m}$	mass flow per second	kg/s
ρ	density	kg/m^3
v	flow speed	m/s
P	pressure	N/ m^2
ΔP_{Res}	pressure difference across restriciton	Pa
ATDC	after top dead centre	
EGR	exhaust gas recirculation	
EGR_{Pos}	EGR valve position	%
f_{EV}	exhaust valve frequency	Hz
H_{Res}	restriction coefficient	
MVEM	mean value engine model	
n	amount of substance	mol
P_{DS}	pressure downstream	Pa
$P_{TurbineAmplitude}$	amplitude of $P_{Turbine}$ pulse	Pa
P_{US}	pressure upstream	Pa
R	gas constant	$J/(mol \cdot K)$
RPM	revolutions per minute	min^{-1}
T	temperature	K
T_{US}	temperature upstream	K
V	volume	m^3
γ	ratio of specific heats	-

Contents

Chapter 1

Introduction

This master thesis problem was devised by Volvo Powertrain, Gothenburg. The modelling was mostly carried out in Lund and the data acquisition was done in Gothenburg.

1.1 Background

Emission legislations are becoming increasingly strict and in order to meet these requirements more and more accurate engine models are needed. In order to lower the NO_x concentration in internal combustion engine emissions, EGR, or Exhaust Gas Recirculation, can be used. EGR recirculates a fraction of the exhaust gas back into the cylinders, thus diluting the intake air. This lowers the maximum combustion temperature and since the formation of NO_x is heavily dependent on temperature the NO_x concentration in emissions is lowered. Thanks to the ability to lower exhaust temperature EGR also prevents Three Way Catalyst, or TWC, damage [Hen99]. On a 13-litre Volvo diesel engine an EGR channel is located between the exhaust and intake manifolds. In order inject EGR gas into the inlet manifold a sufficiently high pressure is needed. This pressure is created by the gas coming out of the exhaust valves and can be controlled with the help of variable turbine blades in the turbo system, so called VGT, Variable Geometry Turbine. The flow through the EGR channel can also be controlled with a poppet valve situated in the EGR channel inlet, the EGR valve. In order to cool the very hot exhaust gases and thus further lowering NO_x concentration, there is also an EGR cooler, a water cooled heat exchanger, in the EGR channel.

The purpose of this master thesis is to model the EGR flow in a Volvo 13-litre diesel engine. The EGR mass flow is currently estimated with a venturi whose estimation is acceptable in general but shows flaws when subjected to pressure pulsations. Volvo assumes that pressure pulsations occur mainly at high torques and low engine speed. The assignment consists of surpassing the current EGR mass flow model and observing the consequences of pressure pulsations with the help of pressure measurements sampled on crank angle basis.

Previous work in this field has been concentrated on mean value engine modelling, or MVEM. MVEM allows modelling of the dominant physical effects without being to complex thus permitting real-time simulation.

1.2 Aims

The master thesis shall deal with the following:

1. Modelling of the EGR flow where the pressure measurements on crank angle basis are input variables. The model should be able to run in real-time.
2. Determine current EGR mass flow estimation error where pressure pulsations are significant. The current venturi mass flow estimation is lacking at high loads and low engine speeds.
3. Establish how fast the pressure should be sampled.
4. If possible, assess where the pressure sensors that measure the driving pressure should be positioned.
5. How do the different cylinders burn? Determine this by looking at pressure.

1.3 Delimitations

The current venturi mass flow estimation shall not be modelled. Its estimated mass flow value will be provided.

1.4 Target group

This report was written for M.Sc. students and employees at Volvo Powertrain.

Chapter 2

Approach

2.1 Project layout

Literature
Literature and master theses in this field were examined.

Measurements
Measurements were performed as many as three times. All measurements were carried out at Volvo, Gothenburg.

Modelling and tuning
The EGR mass flow model was created and tuned.

Venturi error model
A model for this error was created and examined.

Assessing good placing of pressure sensors and cylinder burn
The EGR flow model was used to model the flow based on different pressure sensors downstream. The cylinder burn was examined.

Validation
Using a separate set of data whenever possible the EGR mass flow models and the venturi estimation model were validated.

Robustness and rate of sampling
Robustness and appropriate rate of sampling were examined

2.2 Measurements

Volvo provided an engine rig for measurements. The engine was a six cylinder 13-litre Volvo diesel engine with VGT, EGR, and intercooler.

Measurements were carried out on three separate occasions. The first data set from Volvo showed signs of being faulty since the pressure drop in the EGR channel was much too low. EGR leakage was suspected of causing this error and it was decided that a new data set should be acquired.

The engine had to be modified to accept new sensors that allowed faster sampling. A new pipe with a socket for the new pressure sensors was added to the EGR channel, between the EGR cooler and venturi. The sensors were fitted according to figure 2.1. The exhaust pressure sensor, $P_{Turbine}$, did protrude significantly on the inner side of the exhaust manifold but its effect on the flow was deemed insignificant.

It was not possible to measure the EGR valve position but it was commonly assumed that the valve was sufficiently fast for the dynamics to be neglected. The identification and validation were therefore based on the desired value. The sampling was based on crank shaft angle and sampled twice every degree. Unfortunately the water cooling failed on one pressure sensor. This was the sensor located after the venturi, and the sensor broke down. This was however the least important sensor since the pressure downstream can be measured with the intake pressure sensor P_{Boost}. The $P_{VenturiAfter}$ sensor was nonetheless replaced by a slow sampling sensor.

The signals were conveyed to a program called Osiris that plotted the signals and also stored data from dynamic runs as well as stationary measurements. Dynamic measurements were stored in case dynamic system identification would be needed. During these dynamic measurements the desired values of the EGR position, the engine load, and engine speed were subjected to step changes and the EGR position also had a pseudo-random binary sequence added to the desired value in order to increase the excitation frequency. Dynamic measurements were also used for dynamic validation.

The real EGR mass flow was measured with exhaust gas analysis equipment. This gas flow measurement had a delay since the exhaust gases had to reach the measurement equipment before being measured. This resulted in the mass flow measurements of the second data set only being valid at stationarity, but were used in dynamic simulations as an approximate reference. Temperature sensors typically have slow dynamics and were not able to measure the fast fluctuations in exhaust temperature. This fact was, to some degree, compensated by the model input which was the mean value from these sensors during one engine cycle. A computer stored a sequence of the desired values in stationarity on condition that a specific signal had been constant for a number of seconds.

A load step was intended to be included in these new stationary measurements in order to increase the amount of dynamic data but this was not always the case owing to synchronisation problems. Due to technical difficulties only 21 stationary points ran and these were therefore the only signals available for validation and identification until a third data set was acquired. The band pass filtered pressure pulses from the second stationary file from the second data set can be seen in figures 2.2 and 2.3. The signals have been filtered with a band pass Butterworth filter with a peak at the exhaust valve frequency. It is noteworthy that the $P_{VenturiAfter}$ sensor, even after having been replaced by a slow sampling rig sensor, was incorrectly tuned and its signal will therefore be left out in figures 2.2 and 2.3. In figure 2.3 it is obvious that the pressure amplitude decreases downstream. The mean pressure drop across the EGR valve and EGR cooler seems to be approximately the same for this EGR valve position. The $P_{EGRCoolerAfter}$-P_{Boost} pressure drop is however great, possibly because of the venturi restriction. In figures 2.2 d) and 2.3 d) the interaction between the exhaust pressure pulses and inlet dittos can be discerned. The pattern thus differs slightly from the pressure patterns upstream. The pressure pulse delay in the EGR channel can be deduced from figure 2.3 e). Note that the pressures have all been measured in different volumes but this has been neglected in the report. This difference is prominent between exhaust manifold and EGR cooler and EGR cooler and inlet manifold.

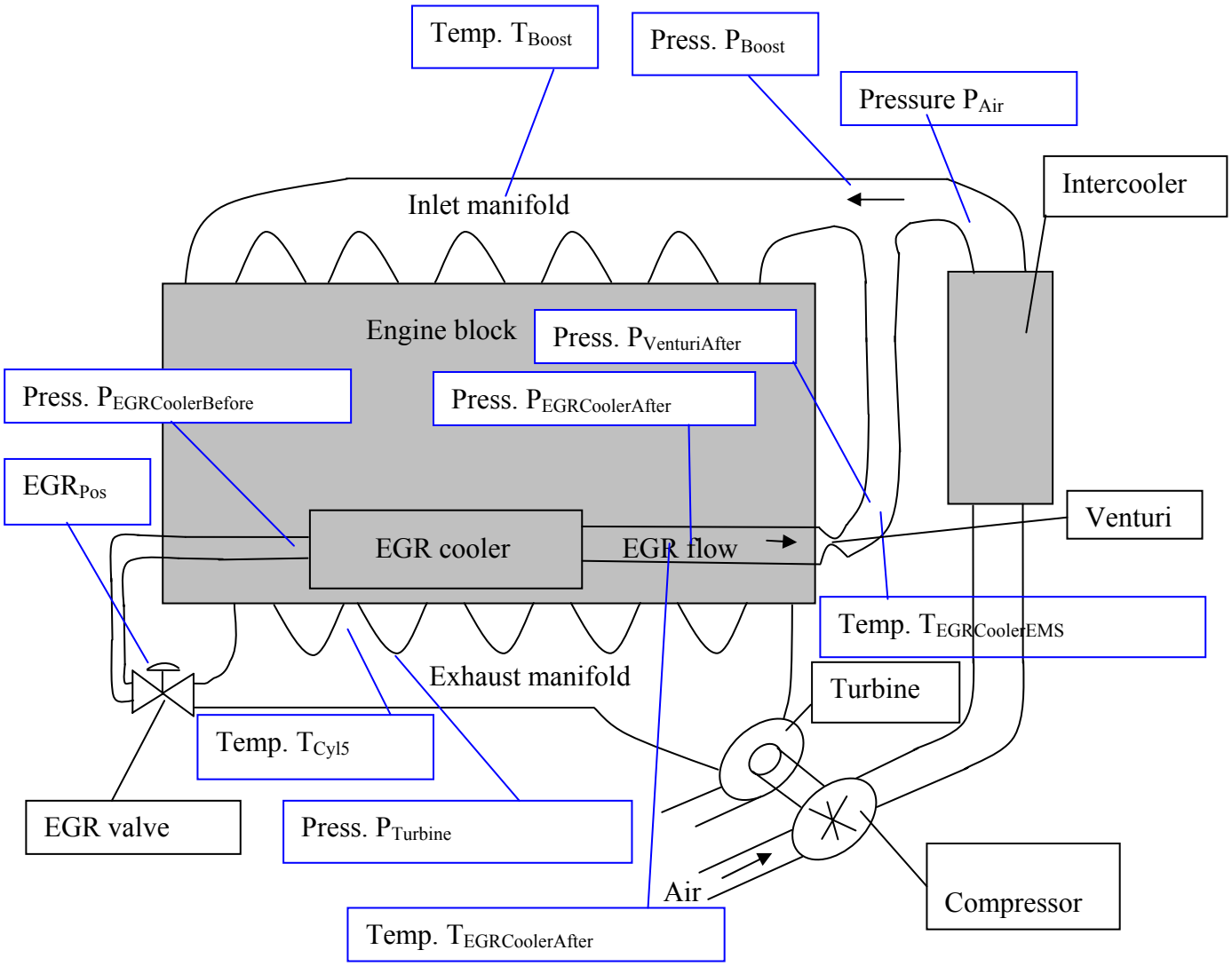

Figure 2.1 The engine and its sensors during acquisition of the second data set.

Table 2.1 Description of measured signals in the second dataset. Some are depicted in figure 2.1.

Signal name	Description
EGR_{Pos}	Position of the EGR poppet valve
P_{Air}	Pressure of inlet air downstream from intercooler
P_{Boost}	Pressure in intake manifold
$P_{EGRCoolerAfter}$	Pressure downstream from EGR cooler but upstream from venturi
$P_{EGRCoolerBefore}$	Pressure downstream from EGR valve but upstream from EGR cooler
$P_{Turbine}$	Pressure in exhaust manifold
T_{Boost}	Temperature in intake manifold
T_{Cyl5}	Exhaust temperature of cylinder five and thereby EGR channel inlet
$T_{EGRCoolerAfter}$	Temperature downstream from EGR cooler and upstream from venturi

A third dataset was acquired to attain a better dynamic rig flow measurement and provide more stationary identification and validation data. This third data set was measured using only standard rig sensors which were assumed to be accurate enough for stationary and slow

dynamic identification and validation. This data set was sampled once every crank angle degree. The stored signals were among others the delayed CO_2 concentrations, see table 2.2, on which the EGR mass flow reference calculation depended. To compensate for the delay in the mass flow reference the CO_2 measurements were examined and the points where they were influenced by the load step were found and the delay assessed. It is noteworthy that the venturi EGR mass flow signal was not included in the third data set and it was therefore impossible to validate the venturi error model using this set. Signals from the third data set are listed in table 2.2.

Table 2.2 Description of signals from the third dataset.

Signal name	Description
CO_{2Conc}	Concentration of CO_2
CO_{2EGR}	CO_2 concentration in inlet manifold
$EGR_{DiffPressEMS}$	Differential pressure across venturi
EGR_{Flow}	Mass flow in EGR channel
EGR_{Pos}	Position of the EGR poppet valve
Flw_{Air}	Flow of air to inlet manifold
Flw_{Fuel}	Flow of fuel
P_{Boost}	Pressure in intake manifold
$P_{Turbine}$	Pressure in exhaust manifold
T_{Boost}	Temperature in intake manifold
T_{Cyl5}	Temperature at cylinder 5 exhaust and thereby EGR channel inlet

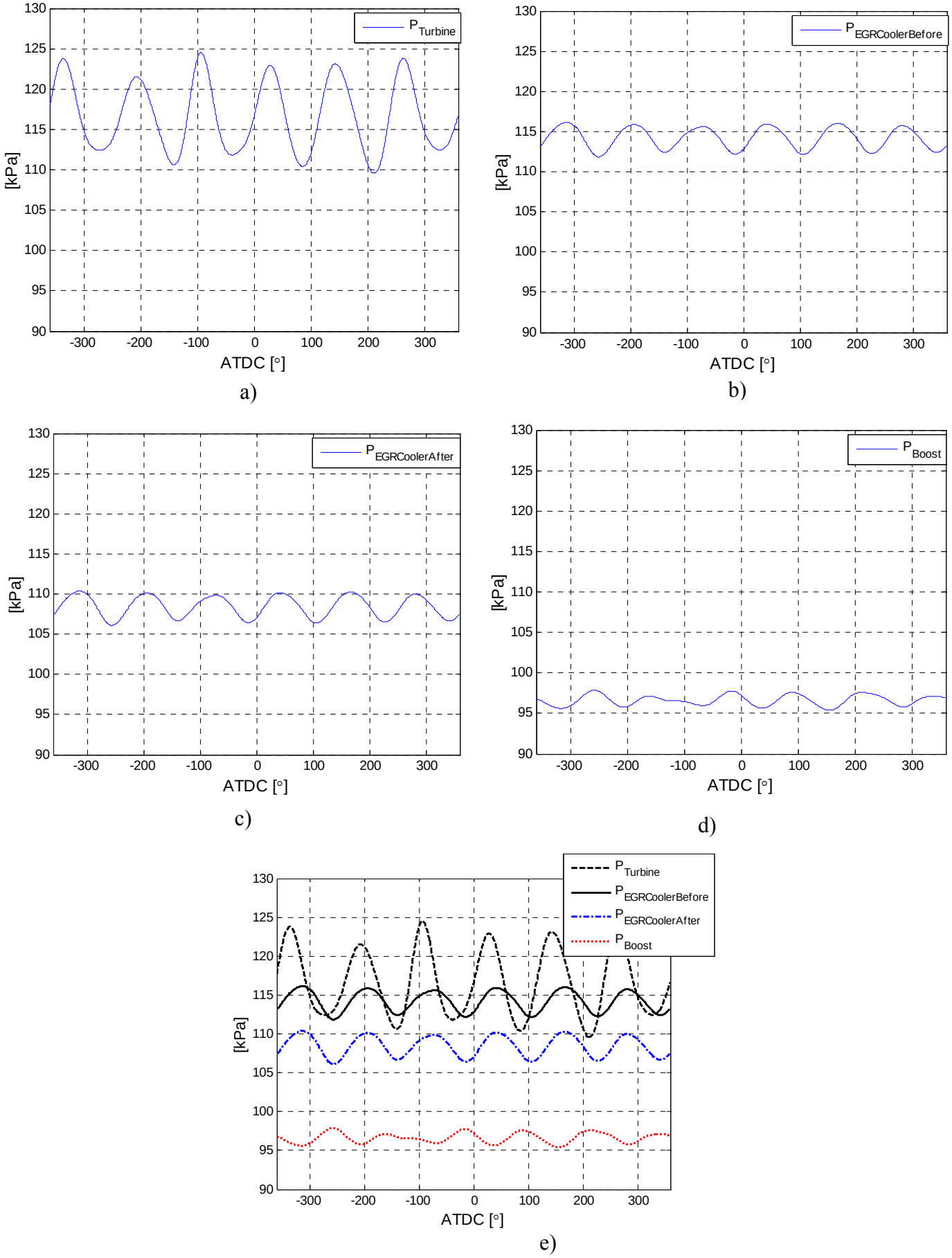

Figure 2.2 Typical filtered pressure pulses from the second data set in stationarity.
a) $P_{Turbine}$ b) $P_{EGRCoolerBefore}$ c) $P_{EGRCoolerAfter}$ d) P_{Boost} e) all pressures

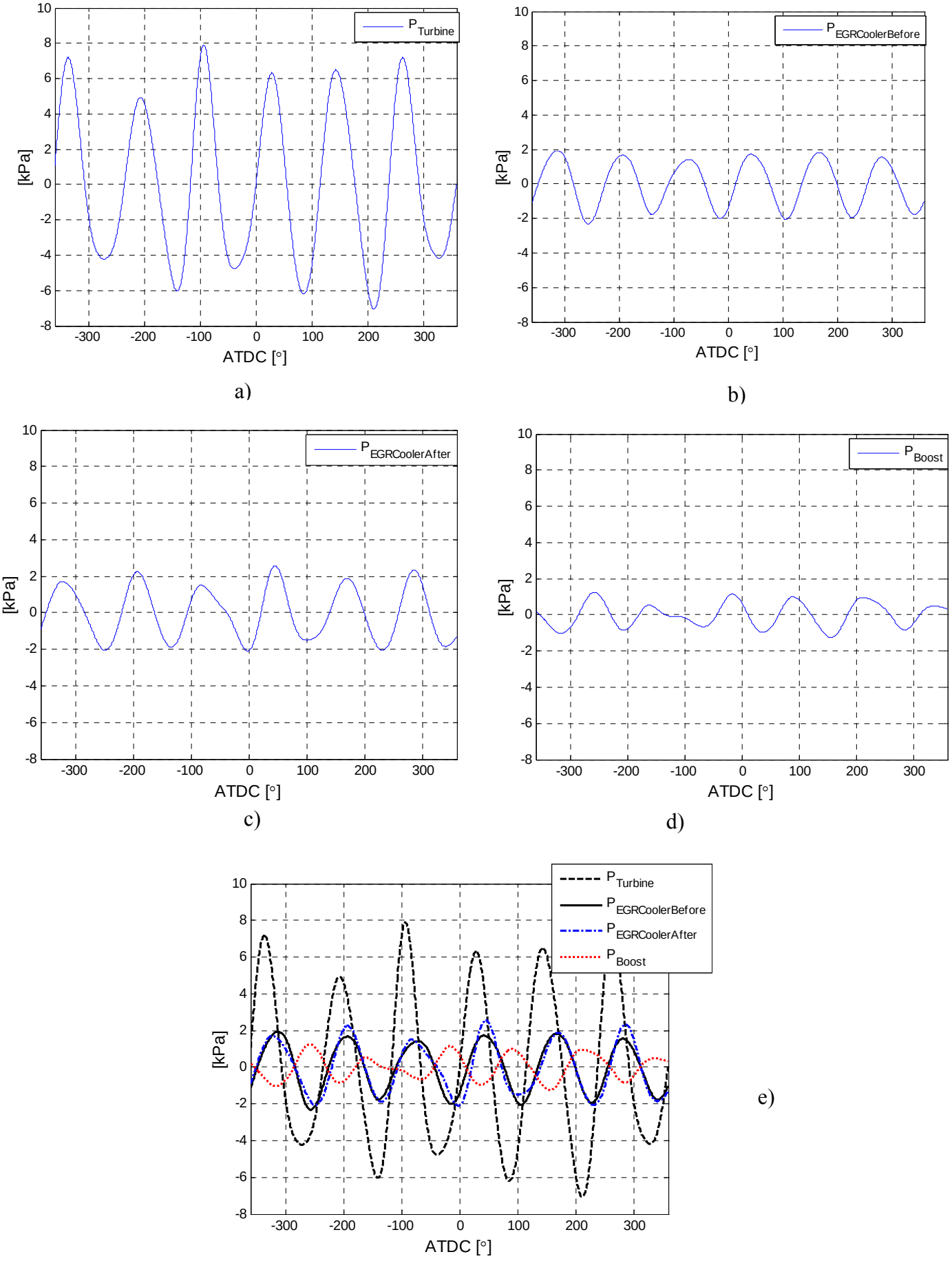

Figure 2.3 Typical filtered and detrended pressure pulses from the second data set in stationarity. a) $P_{Turbine}$ b) $P_{EGRCoolerBefore}$ c) $P_{EGRCoolerAfter}$ d) P_{Boost} e) All signals

Chapter 3

Modelling

3.1 EGR mass flow

In order to model the EGR mass flow equation (3.1) for steady-state flow through poppet valves from Heywood, [Hey88] page 226, was used.

$$\dot{m} = A_{EGR} \frac{P_{US}}{\sqrt{T_{US} \cdot R}} \psi\left(\frac{P_{DS}}{P_{US}}, \gamma\right)$$

$$\psi\left(\frac{P_{DS}}{P_{US}}, \gamma\right) = \begin{cases} \sqrt{\frac{2\gamma}{\gamma - 1}\left(\left(\frac{P_{DS}}{P_{US}}\right)^{\frac{2}{\gamma}} - \left(\frac{P_{DS}}{P_{US}}\right)^{\frac{\gamma+1}{\gamma}}\right)} & \text{if } \frac{P_{DS}}{P_{US}} \geq \left(\frac{2}{\gamma+1}\right)^{\frac{\gamma}{\gamma-1}} \\ \sqrt{\gamma\left(\frac{2}{\gamma+1}\right)^{\frac{\gamma+1}{\gamma-1}}} & \text{else} \end{cases} \quad (3.1)$$

where γ is the ratio of specific heats, P_{DS} and P_{US} are the pressures downstream and upstream respectively. T_{US} is the pressure upstream and A_{EGR} is the effective area. The "else" case in equation (3.1) never held true for the stationary and dynamic data and this equation was therefore omitted from the modelling. In order to assess the effective area A_{EGR} in equation (3.1) a second degree function of the EGR valve position was used according to Ericson [Eri04]. This was justified with the assumption that the valve at small valve lifts will have an area that is a linear function of valve lift. It was also assumed that the valve area will be described well by a quadratic function at higher lifts since the area will be limited mainly by the stem holding the valve tulip. A poppet valve and its seat can be seen in figure 3.1.

$$A_{EGR} = k_1 + k_2 \cdot EGR_{Pos} + k_3 \cdot EGR_{Pos}^2 \quad (3.2)$$

To further minimise the error this model was in turn increased with a look-up table offset added to equation (3.1) under the square root.

$$\text{offset} = f(P_{Turbine}, f_{EV}) \quad (3.3)$$

This offset had the pressure upstream, $P_{Turbine}$, and exhaust valve frequency, f_{EV}, as input data.

Moreover, a look-up table similar to (3.3) was suggested by Volvo, but this model was based on exhaust valve frequency and the exhaust pressure pulsation amplitude, that was extracted manually. In order to deduce this amplitude $P_{Turbine}$ was band pass filtered around the exhaust valve frequency to exclude noise and then minimum and maximum pressures were found and pressure pulsation amplitude calculated. This procedure was repeated for all stationary measurements from the second data set and the data was used to derive the look-up table. The look-up table can be seen in figure 3.4.

$A_{EGRCompLU} = f(P_{TurbineAmplitude}, f_{EV}) \cdot A_{EGR}$ (3.4)

To further improve equation (3.1) a compensation was multiplied by A_{EGR}, disregarding the look-up tables that had been developed, according to Ericson [Eri04].

$A_{EGRComp} = f(P_{US}, P_{DS}, EGR_{Pos}) \cdot A_{EGR}$ (3.5)

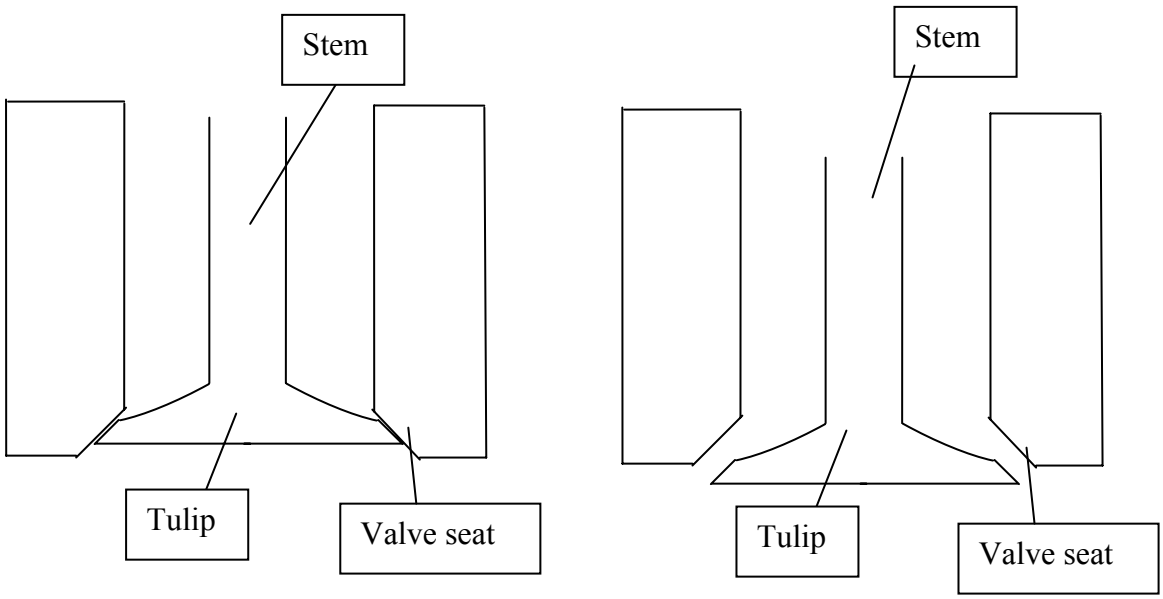

Figure 3.1 From the left: closed and open poppet valve.

The engine was equipped with VGT that could be adjusted but this would only have changed the driving pressure and hence the VGT did not have to be included in the model.

A model based on an incompressible flow was also tested according to [Höc06], see equation (3.6).

$$\dot{m} = \sqrt{\frac{P_{US} \cdot \Delta P_{\mathrm{Res}}}{H_{\mathrm{Res}} \cdot T_{US}}} \tag{3.6}$$

which can be linearised to

$$\dot{m} = \sqrt{\frac{P_{US}}{H_{\mathrm{Res}} \cdot T_{US}}} \cdot \frac{\Delta P_{\mathrm{Res}}}{\sqrt{P_{Lin}}} \text{ where } 0 \le \Delta P_{\mathrm{Res}} \le P_{Lin} \tag{3.7}$$

where H_{Res} is a restriction coefficient, P_{US} is the pressure upstream, P_{DS} is the pressure downstream, and T_{US} is the temperature upstream.

Research at Volvo has shown a linear relationship between exhaust pressure amplitude and exhaust mass flow. If this relationship is valid in the EGR channel a measurement of the pressure amplitude might be used to assess the mass flow.

3.2 Venturi mass flow estimation error

The venturi mass flow estimation is based on the difference in pressure between venturi inlet and outlet. The venturi can be seen in figure 3.2. The venturi itself is a cone-shaped restriction which results in this aforementioned pressure difference. To estimate the venturi estimation error, stationary data from the second data set was used since the engine rig mass flow measurement was somewhat unreliable during transients. The error in percent was calculated and plotted versus engine speed and load. A surface was fitted to the errors.

Previous studies at Volvo have concluded that pressure pulse amplitude is proportional to the mass flow in the exhaust. If this also holds true in the EGR channel and if the venturi estimate is at its worst during severe pressure pulses then maybe a linear relationship can be found between mass flow and venturi mass flow estimation error.

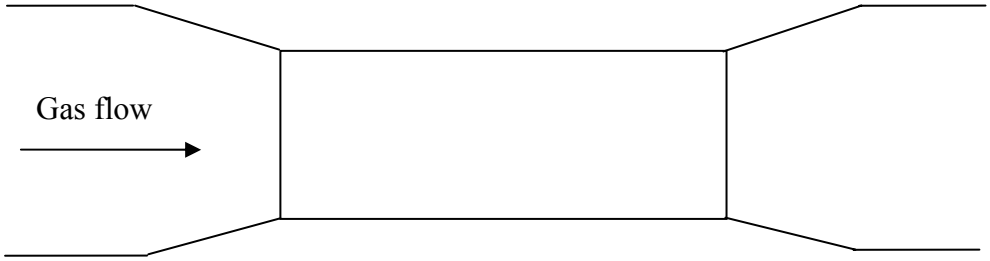

Figure 3.2 The venturi.

Chapter 4

Model identification and results

Least-squares identification was used to a great extent during the modelling procedure, see [Joh06] or [Gla91]. The models were identified and validated using the mean relative error and the maximum relative error according to a paper, [Höc06].

$$\text{Mean relative error} = \frac{1}{N}\sum_{i=1}^{N}\frac{\left|\hat{x}(t_i)-x(t_i)\right|}{\left|x(t_i)\right|} \tag{4.1}$$

$$\text{Maximum relative error} = \max_{1\le i\le N}\frac{\left|\hat{x}(t_i)-x(t_i)\right|}{\left|x(t_i)\right|} \tag{4.2}$$

where $\hat{x}$ means modelled value and x is the reference measurement.

4.1 EGR mass flow

The goal of the EGR mass flow modelling was to surpass the accuracy of the venturi mass flow estimation and consequently the estimation was compared with the venturi ditto throughout the modelling and tuning procedures whenever possible. Stationary points were used for identification since the engine rig mass flow measurement was filtered and had a delay that could only be compensated to some degree of accuracy. Furthermore it was commonly assumed at Volvo that the rig mass flow measurement was heavily filtered making dynamic validation difficult. Also equation (3.1) is, according to Heywood [Hey88], valid only in stationarity. It was however assumed that the model would be able to handle slow dynamics.

A look-up table can not deal with values outside the identification data range unless extrapolated whereas models estimated with least-squares estimation will at least give approximate values for data points that in fact lay outside the data range that was used to identify the model.

Identification of the model based on equations (3.1) and (3.2) using the third data set gave the coefficients in table 4.1.

Table 4.1 Coefficients in equation (3.2).

Constant	Value
k_1	$-3.466320801708\cdot10^{-5}$
k_2	$2.1101371368877\cdot10^{-5}$
k_3	$-7.953704172306001\cdot10^{-5}$

To further improve accuracy, the look-up table (3.3) was used. It can be seen in figure 4.1.

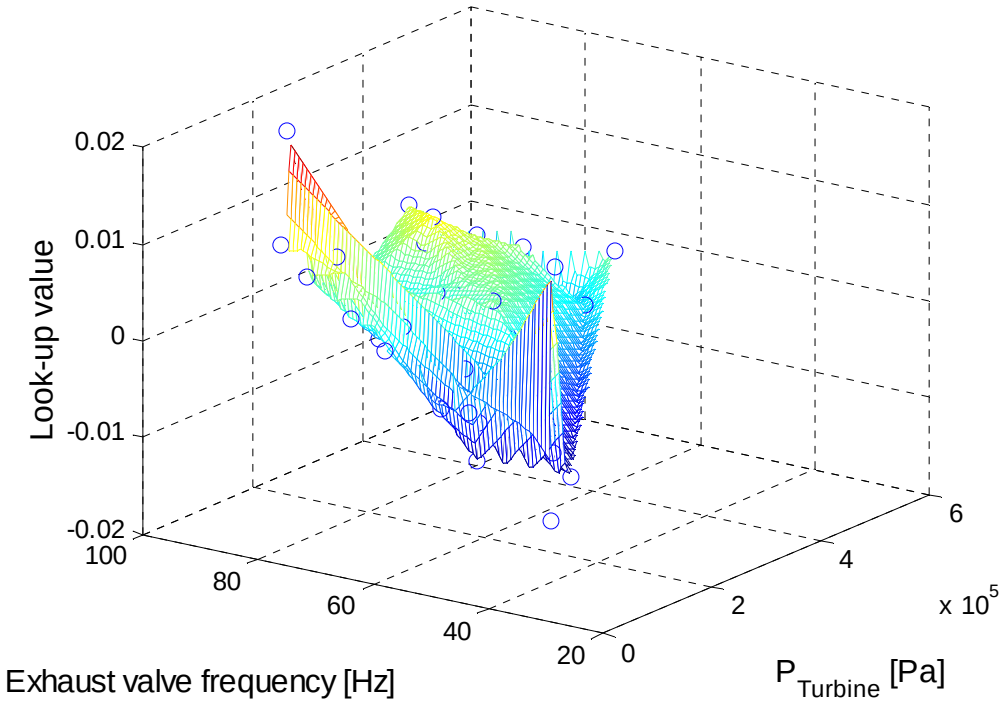

Figure 4.1 Look-up table (3.3).

In order to check Volvos suggestion, look-up table (3.4) was identified to make up $A_{EGRCompLU}$. The identification of this look-up table was performed using equation (3.2) with the values from table 4.1 and thereby the third data set. Only ten stationary points were available for identification of the look-up table, since a look-up table needs validation data for validation. Look-up table (3.4) can be seen in figure 4.2.

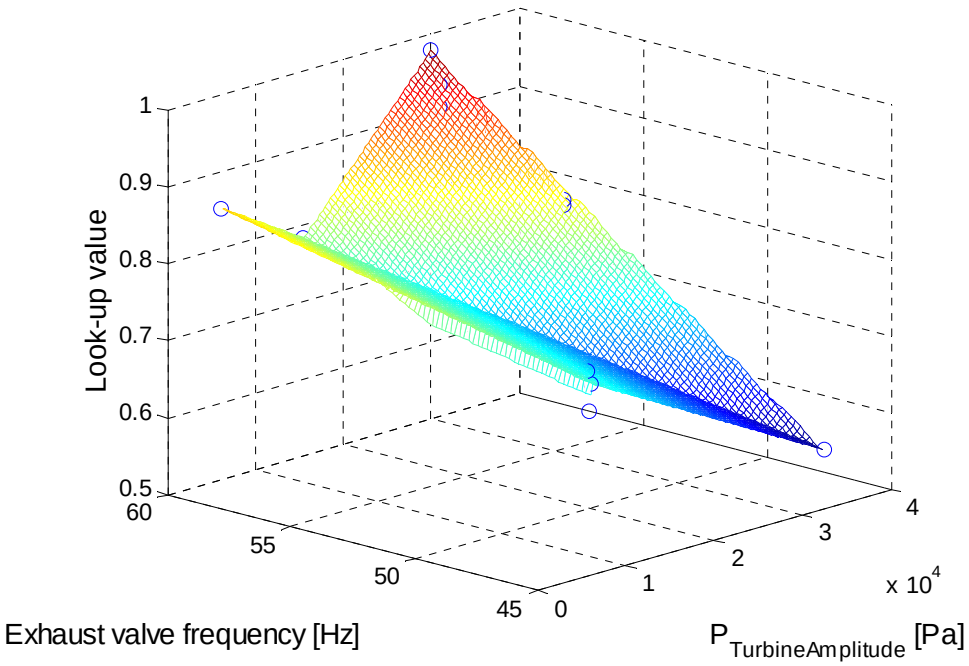

Figure 4.2 Look-up table (3.4).

Ignoring the aforementioned look-up tables, equation (3.5) was identified using least-squares estimation, and the constants for two promising versions can be seen in tables 4.2 and 4.3. The equations themselves are shown in equations (4.3) and (4.4).

$$A_{EGRComp} = (k_1+k_2 \cdot P_{Turbine}+k_3 \cdot P_{Boost}+k_4 \cdot EGR_{Pos}) \cdot A_{EGR} \quad (4.3)$$

$$A_{EGRComp} = (k_1+k_2 \cdot P_{Turbine}+k_3 \cdot P_{Turbine}^2+k_4 \cdot P_{Boost}+k_5 \cdot P_{Boost}^2+k_6 \cdot EGR_{Pos}) \cdot A_{EGR} \quad (4.4)$$

Table 4.2 Coefficients in equation (4.3).

Constant	Value
k_1	0.96834449808627
k_2	$4.2720455 \cdot 10^{-7}$
k_3	$-3.1191852 \cdot 10^{-7}$
k_4	$-6.2837725281 \cdot 10^{-4}$

Table 4.3 Coefficients in equation (4.4).

Constant	Value
k_1	0.60703030251395
k_2	$-4.64702822 \cdot 10^{-6}$
k_3	$5.77 \cdot 10^{-12}$
k_4	$9.57001221 \cdot 10^{-12}$
k_5	$-1.636 \cdot 10^{-12}$
k_6	-0.04362427766842

Equations (3.6) and (3.7) were tested on the EGR cooler restriction, according to [Höc06]. The restriction coefficient H_{Res} was identified using mean calculation for stationary data. This model showed bad correspondence to the rig flow during identification and did very poorly in stationary tests. The equations (3.6) and (3.7) were tested with equally bad results. The restriction was therefore changed since equation (3.6) is only valid for constant energy systems and the EGR cooler was suspected of not fulfilling the constant energy assumption. The only other constant area restriction was the venturi. Pressure $P_{EGRCoolerAfter,}$ P_{Boost} and $T_{EGRCoolerAfter}$ were chosen as signals and a natural model extension was the adoption of a least-squares estimated function that replaced the restriction constant H_{Res}. By plotting H_{Res} versus different signals it was concluded that the following might work.

$$H_{Res}=(k_1+k_2 \cdot (P_{EGRCoolerAfter} - P_{Boost})+k_3 \cdot P_{EGRCoolerAfter}+k_4 \cdot P_{EGRCoolerAfter}^2) \quad (4.5)$$

The latter equation did much to improve model performance. The constants in equation (4.5) can be seen in table 4.4.

Table 4.4 Constants in equation (4.5).

Constant	Value
k_1	$-6.93036973380001 \cdot 10^{10}$
k_2	$0.00041905041180 \cdot 10^{10}$
k_3	$0.00002913891279 \cdot 10^{10}$
k_4	$0.00000000004588 \cdot 10^{10}$

In order to assess whether there is a linear connection between EGR mass flow and the amplitude in the exhaust manifold, $P_{TurbineAmplitude}$ was plotted versus mass flow. The result can be seen in figure 4.3.

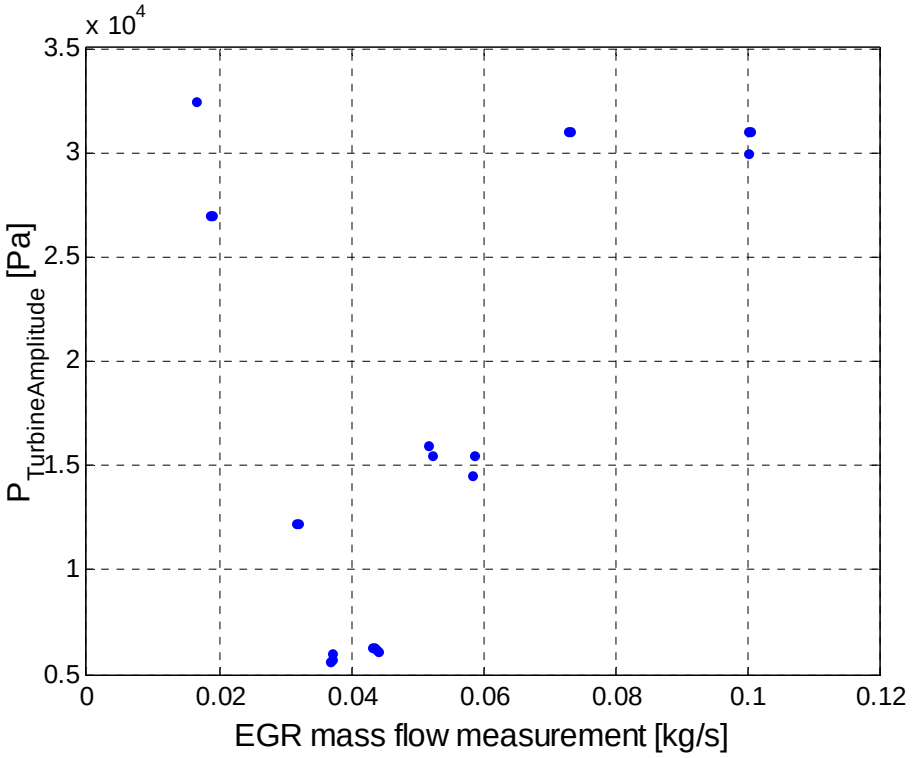

Figure 4.3 Exhaust manifold pressure amplitude versus EGR mass flow.

4.2 Venturi mass flow estimation error

This subchapter will be excluded and presented in an appendix reserved for Volvo due to Volvo internal policy.

4.3 Assessing how cylinders burn

In order to derive the way cylinders burn, the temperature at the exhaust valve of cylinder five, T_{Cyl5}, was measured and so was the pressure at the EGR channel inlet, $P_{Turbine}$. These signals from the second data set were sampled twice every crank angle degree. The dynamics of temperature sensors are typically slow and not able to capture a physical quantity that fluctuates as fast as exhaust peak temperatures induced by valve opening. The same opening results in pressure peaks six times every two crank angle revolutions. The temperature at every exhaust valve should be able to characterise the manner in which the specific cylinder burns, but sadly only the aforementioned slow temperature sensor was available and each temperature peak may be distorted on the way to the sensor. The pressure and temperature may be related to each other using the ideal gas law, as seen in equation (4.6).

$$P \cdot V = n \cdot R \cdot T \tag{4.6}$$

$P_{Turbine}$ and T_{Cyl5} during half an engine cycle can be seen in figure 4.4. The signals are noisy and it is hard to tell whether there is a connection. In order to isolate the effects caused by the exhaust valve frequency and reduce noise the pressure and temperature signals were filtered around this frequency using a band pass Butterworth filter with a peak at this frequency. The filtered temperature and filtered pressure signals can be seen in figure 4.5. The coherence between these signals is depicted in figure 4.6.

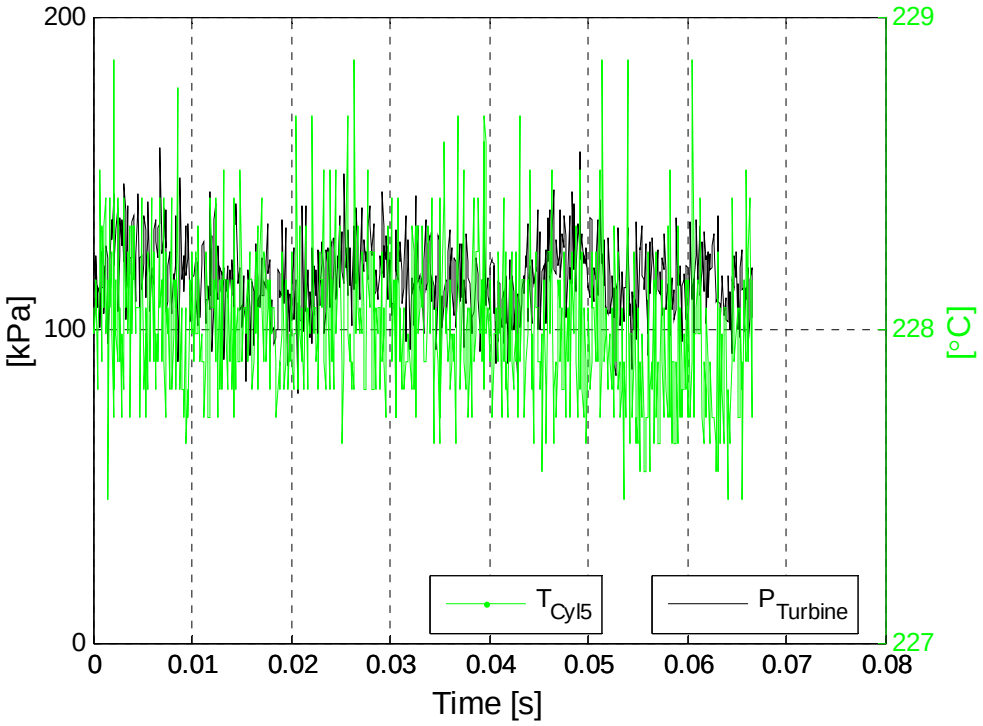

Figure 4.4 T_{Cyl5} and $P_{Turbine}$ during half a cycle.

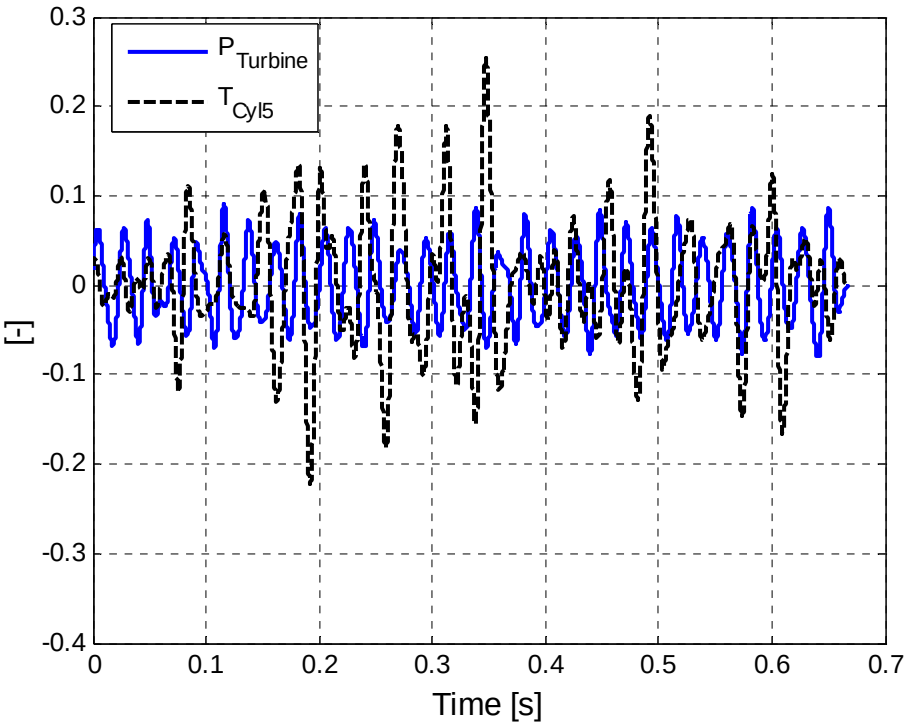

Figure 4.5 $P_{Turbine}$ and T_{Cyl5} in stationary measurement. The signals have been detrended and filtered with Butterworth filter around the exhaust valve frequency.

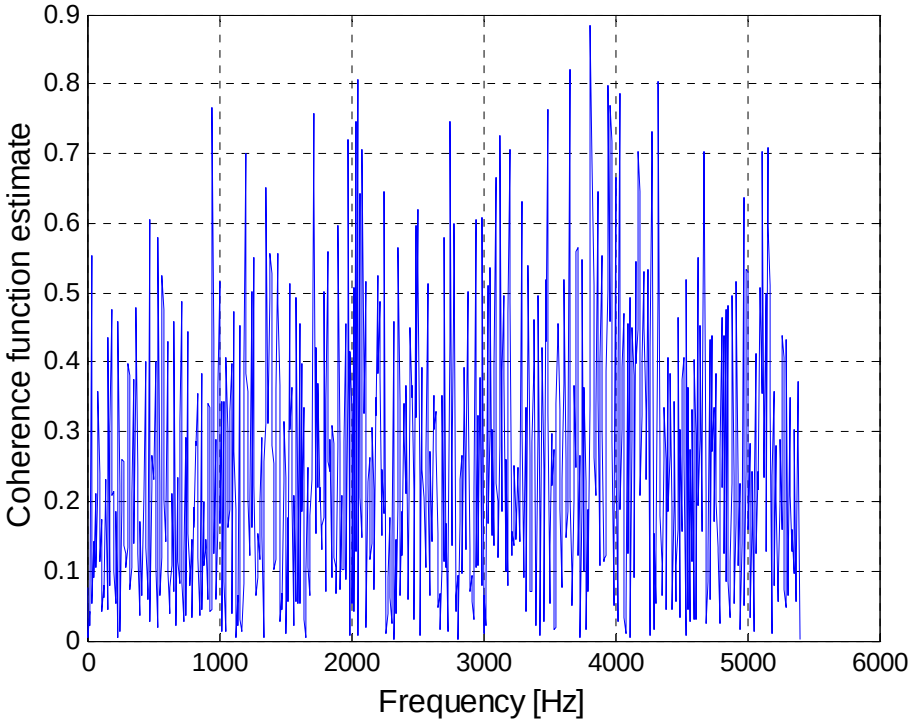

Figure 4.6 Coherence for $P_{Turbine}$ and T_{Cyl5}.

4.4 Finding appropriate position of driving pressure sensors

Finding fitting placing of pressure sensors was rather difficult and there is no guaranteeing that the best placement was found since the assessment was based on the available pressure sensors in figure 2.1. Furthermore the pressure drop across the EGR valve was always included in the model and therefore the upstream pressure was always the intake manifold pressure $P_{Turbine}$. The flow was modelled with equation (3.1) and the downstream pressure changed between available pressure sensors. Each combination of pressure sensors had its own set of least-squares estimated vectors and the corresponding compensations can be seen in the following equations

$$A_{EGR} = k_1 + k_2 \cdot EGR_{Pos} + k_3 \cdot EGR_{Pos}^2 \quad (4.7)$$

$$A_{EGRComp} = (k_1 + k_2 \cdot P_{US} + k_3 \cdot P_{US}^2 + k_4 \cdot P_{DS} + k_4 \cdot P_{DS}^2 + k_4 \cdot EGR_{Pos}) \cdot A_{EGR} \quad (4.8)$$

The aforementioned combinations of pressures were used in the mean value model and the estimated mass flow was compared to that of the rig measurement. The pressures were only compared with stationary identification data since too few data points were available. Also a model that does not describe the identification data correctly may have even greater difficulties during validation. The comparison methods used were the mean and maximum relative errors according to equations (4.1) and (4.2).

Table 4.5 Maximum and mean relative errors for different pressure combinations.

	$P_{Turbine}$-P_{Boost}	$P_{Turbine}$-$P_{EGRCoolerBefore}$	$P_{Turbine}$-$P_{EGRCoolerAfter}$
Maximum relative error (%)	17.53	49.87	16.47
Mean relative error (%)	4.66	13.89	5.56

As can be seen in table 4.5 the measurement involving $P_{Turbine}$ and $P_{EGRCoolerAfter}$ has the smallest maximum relative error. Note that this data was available too late in the work process due to data error. The modelling was therefore based on $P_{Turbine}$-P_{Boost}.

4.5 Robustness and fitting sampling intervals

In order to assess how a pressure error changes the mass flow estimation, equation (3.1) combined with equations (3.2) and (4.4) were subjected to pressure errors. This error was related to a mass flow error in percent. The error definition is as follows

$$\text{Mass flow error} = (\dot{m}_{POffset} - \dot{m}) / \dot{m} \quad (4.9)$$

An error limit of ±10 % was assumed to be an acceptable mass flow error. Since the mass flow error depends on other parameters than P_{Boost} and $P_{Turbine}$ the error curves in figure 4.6 will differ between stationary points with different temperatures and EGR positions. The data in figure 4.6 e) and f) is the worst case data for the validation data set because of an unprecedented small pressure drop. It is therefore reasonable to use this data to consider what a minimum rate of sampling may be.

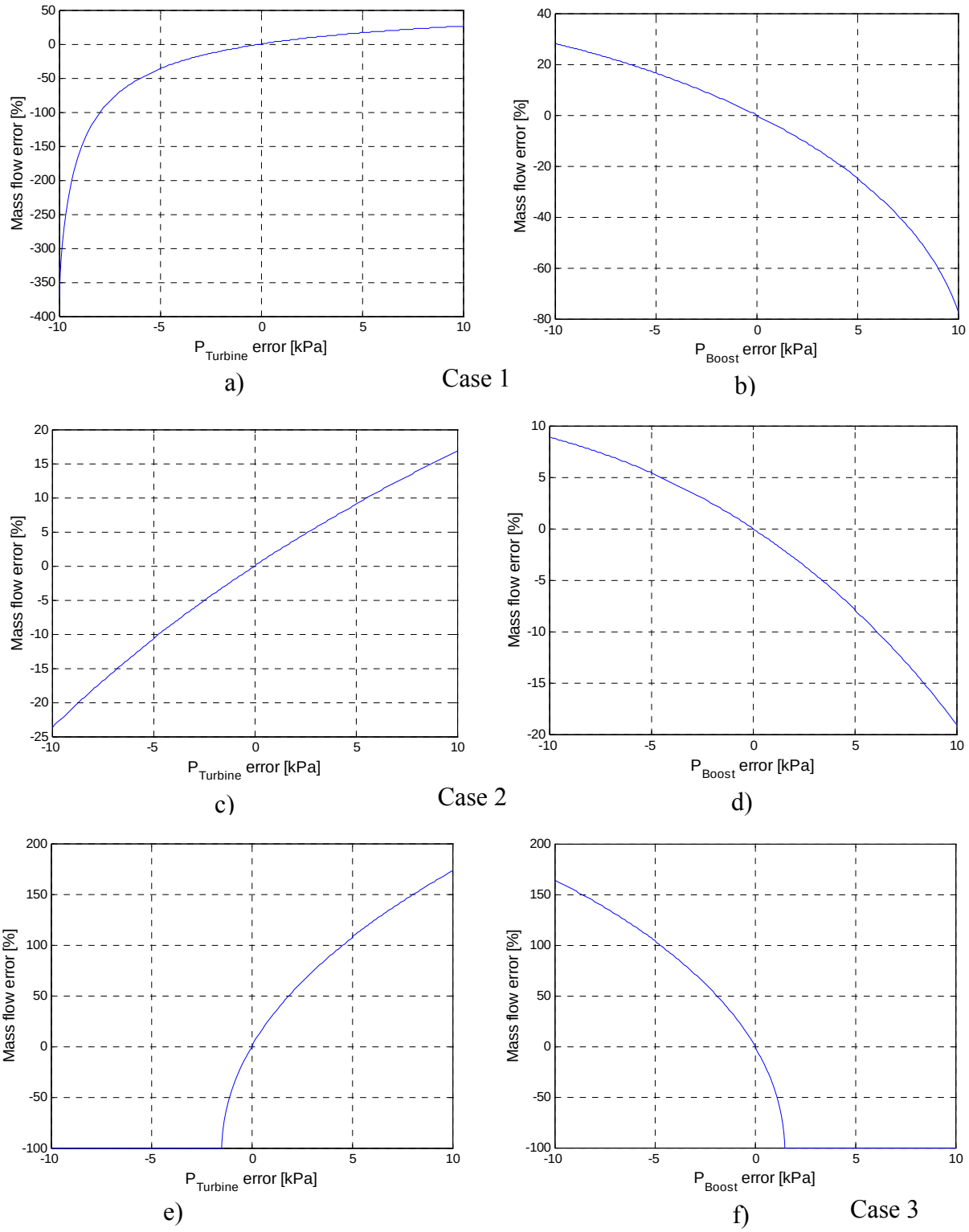

Figur 4.6 a)-b), c)-d), and e)-f) show errors for three engine cycles at different operating points.

The straight lines appearing in figure 4.6 e) and f) are the result of too high an error in P_{Boost} and $P_{Turbine}$ which will result in an imaginary mass flow in equation (3.1). This is highly unwanted but a mass flow error of -10 % occurs already at 0.250 kPa.

To depict the results from the plots above a table was devised for these three operating points using the same mass flow estimation equations.

Table 4.6 Errors for different operating conditions.

Case	RPM [min^{-1}]	Load [Nm]	$P_{Turbine}$ error [kPa]	P_{Boost} error [kPa]	$P_{Turbine}$ error [%]	P_{Boost} error [%]	EGR flow error [%]
1	1400	1400	10	0	6.36	0	35.8
	1400	1400	-10	0	-6.36	0	-78.71
	1400	1400	0	10	0	6.81	-77.64
	1400	1400	0	-10	0	-6.81	28.23
2	1400	605	10	0	6.68	0	16.82
	1400	605	-10	0	-6.68	0	-23.81
	1400	605	0	10	0	7.82	-19.10
	1400	605	0	-10	0	-7.82	8.89
3	800	1000	10	0	4.81	0	173.09
	800	1000	-10	0	-4.81	0	imag.
	800	1000	0	10	0	4.84	imag.
	800	1000	0	-10	0	-4.84	164.5

In order to assess how fast a sampling that is needed in order to give an accurate enough moving average signal as input to equation (3.1) combined with equations (3.2) and (4.4) a maximum allowed pressure error was assessed from robustness plot 4.6. Figure 4.7 shows the resulting pressure error after resampling the pressures used in figures 4.6 e) and f). This pressure error can be related to a specific sample rate and give an indication of what a minimum sampling rate might be. Figure 4.7 shows the rate of resampling during one engine cycle. The maximum error between P_{Boost} data points and the mean calculation of P_{Boost} was 6.65 kPa and the $P_{Turbine}$ ditto was 1.23 kPa. The error definitions used when resampling inputs can be seen in equations (4.10) and (4.11).

$$\text{Pressure error}=\text{mean(PResampled)}-\text{mean(P)} \tag{4.10}$$

$$\text{Mass flow error} = (\dot{m}_{\text{EstimatedResampled}} - \dot{m}_{\text{Estimated}}) / \dot{m}_{\text{Estimated}} \tag{4.11}$$

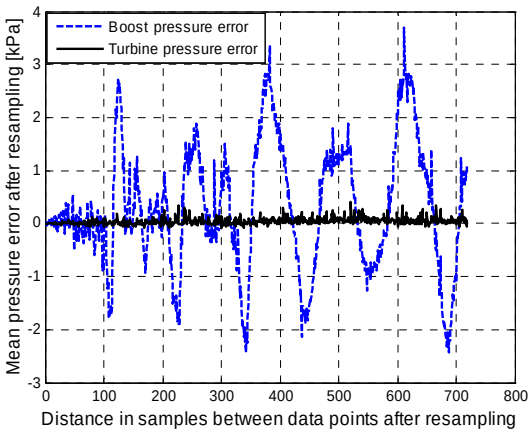

Figure 4.7 The result of resampling the pressures from plots 4.6 e) and f).

The robustness plots above are only valid if only one of the pressures in the model changes. A more realistic assumption is that the moving average means of all signals change when resampling. In order to investigate this effect on the mass flow from figure 4.6 e) and f) all signals were resampled and the deviation from the original mass flow estimate was examined.

The result can be seen in figure 4.8. A similar test was devised where only the pressures were resampled simultaneously. This plot was almost identical to figure 4.8.

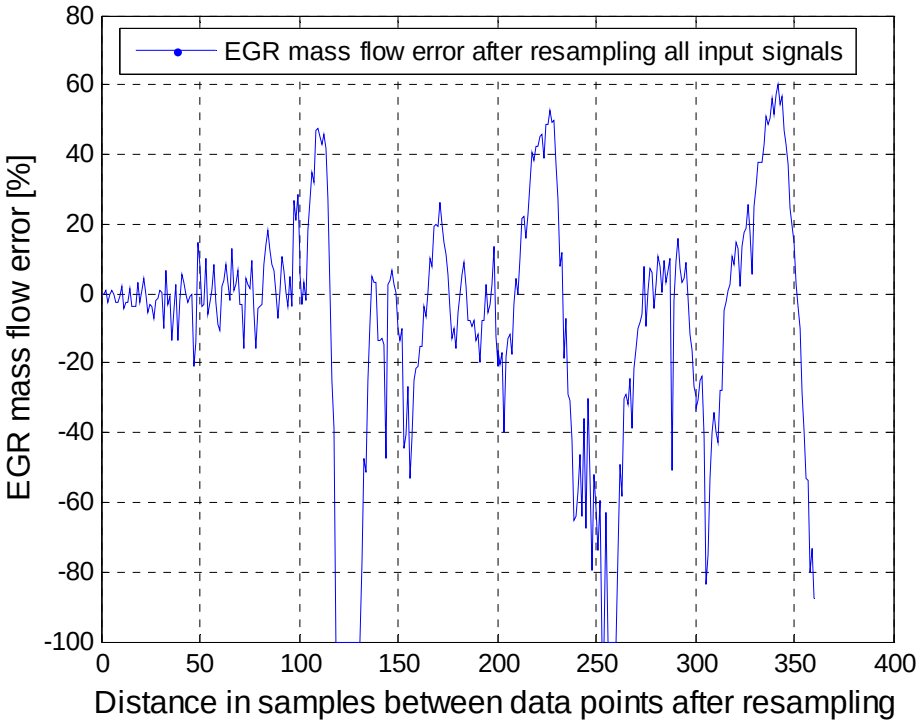

Figure 4.8 Mass flow error when resampling all input signals.

Chapter 5

Model validation

Stationary measurements were used to a large extent when validating the models since the dynamic rig measurement behaviour is heavily filtered. Equation (3.1) and the other suggested models only apply to and have only been identified for stationary flow and it is therefore interesting to see how well they will perform during transients. It was clear that a slightly worse stationary performance was accepted if the model performed better dynamically. The third data set provided the means to compensate for delays in CO_2 measurements, thus allowing more accurate rig mass flow measurement behaviour. This compensation was not able to counter weigh the filtered measurements, that is fast mass flow fluctuations were not necessarily depicted in the mass flow measurement.

Dynamic validation was by calculation of the variance accounted for value according to [Joh06].

$$\tau_{VAF} = (1 - \frac{(y_N - \hat{y}_N)^T (y_N - \hat{y}_N)}{y_N{}^T y_N}) \cdot 100 \ [\%] \tag{5.1}$$

where y_N is the real value and $\hat{y}_N$ is the estimated value. Since the reference measurement was filtered the most accurate way of affirming the model correctness may however be to look at the corresponding pressures and EGR position.

5.1 EGR mass flow

The models in chapter 5.1 are validated with a part of the third data set different from the third data set identification data, unless stated otherwise. The third data set contains reliable data even if the sensors are less accurate than the ones in the second data set.

Using only equations (3.1) and (3.2), the mass flow estimation was validated and the result can be seen in figures 5.1 and 5.2. When using histograms to assess error the ideal case is a gathering of bars around zero percent.

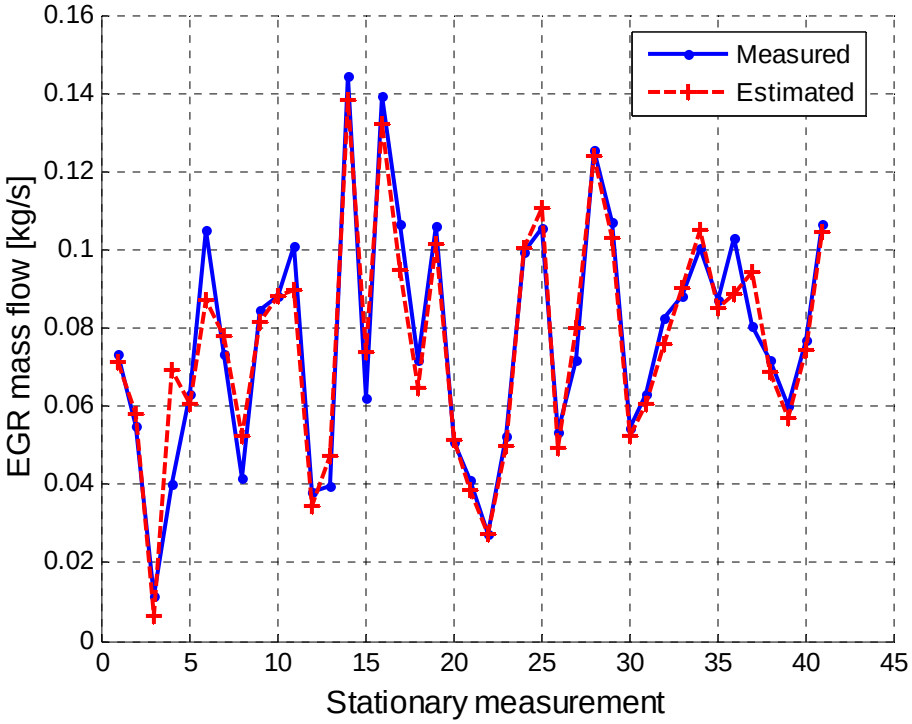

Figure 5.1 Estimated mass flow using (3.1) and (3.2).

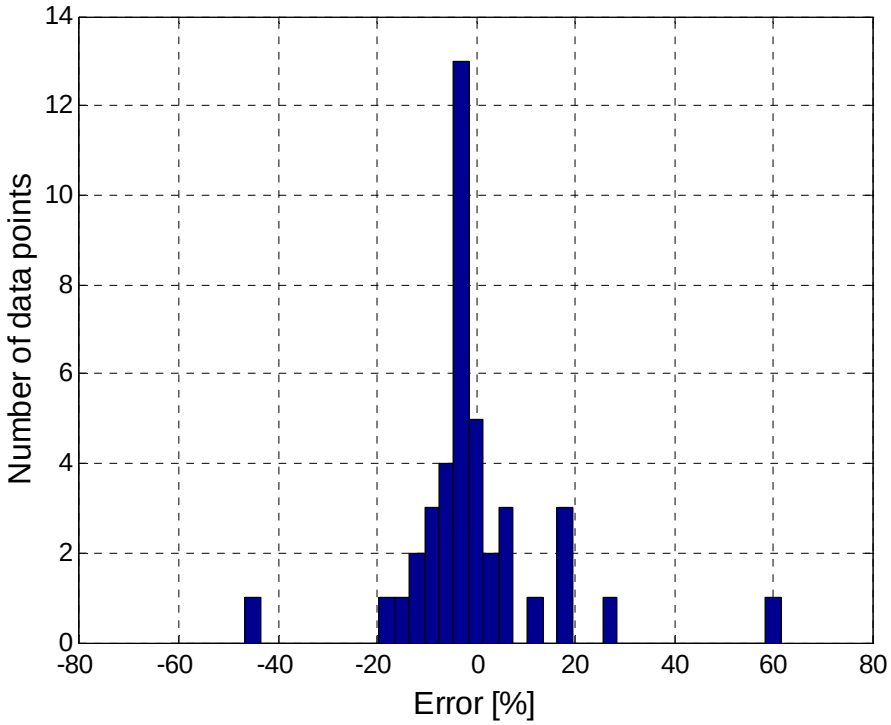

Figure 5.2 Errors for equations (3.1) and (3.2).

Using equations (3.1), (3.2), and (3.5), the latter in the guise of equation (4.3), the mass flow was once again validated with stationary data, see figures 5.3 and 5.4.

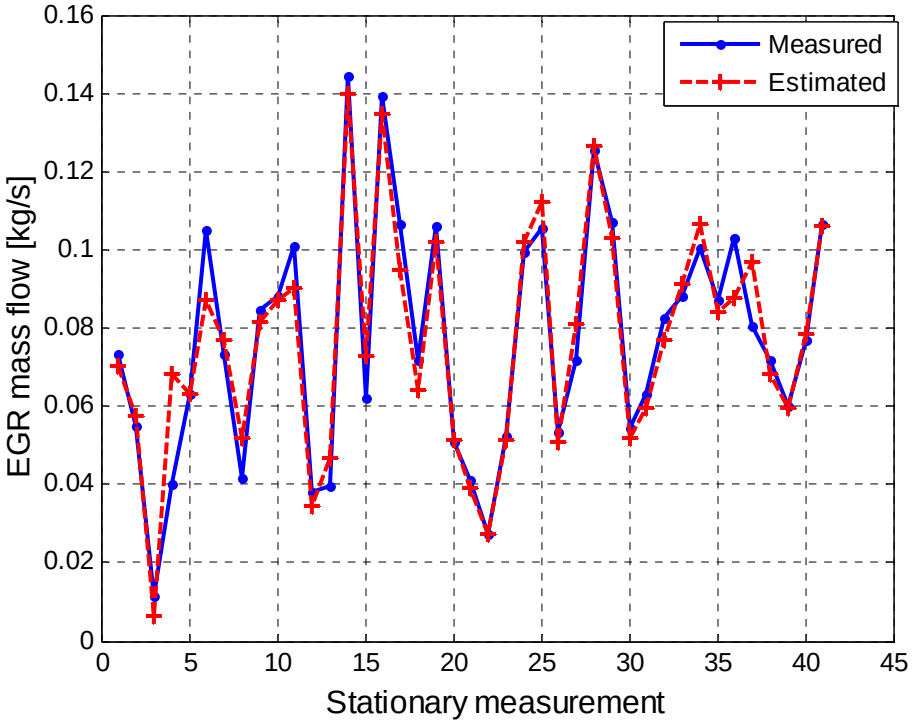

Figure 5.3 Mass flow estimation using equations (3.1), (3.2), and (4.3).

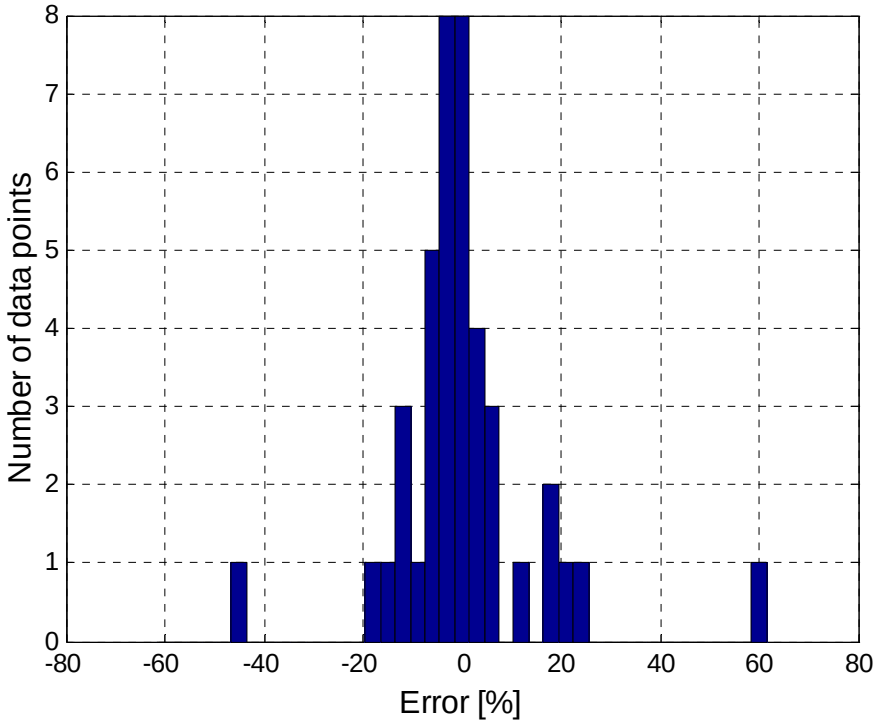

Figure 5.4 Errors using (3.1), (3.2), and (4.3).

Equations (3.1), (3.2), and the extended version of equation (3.5), equation (4.4), were used in figures 5.5 and 5.6.

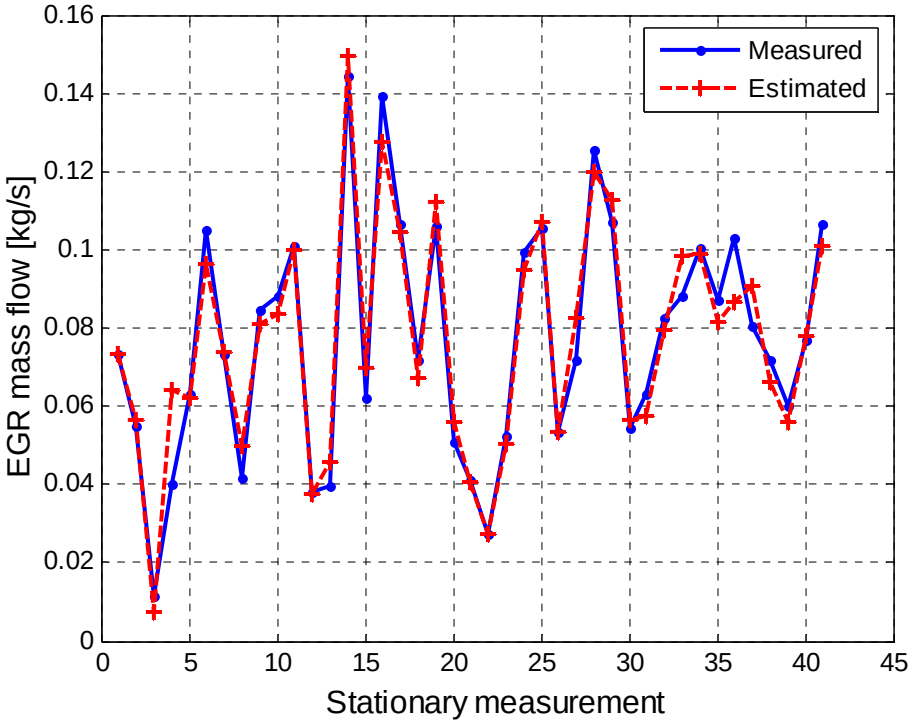

Figure 5.5 Mass flow estimation using equations (3.1), (3.2), and (4.4)

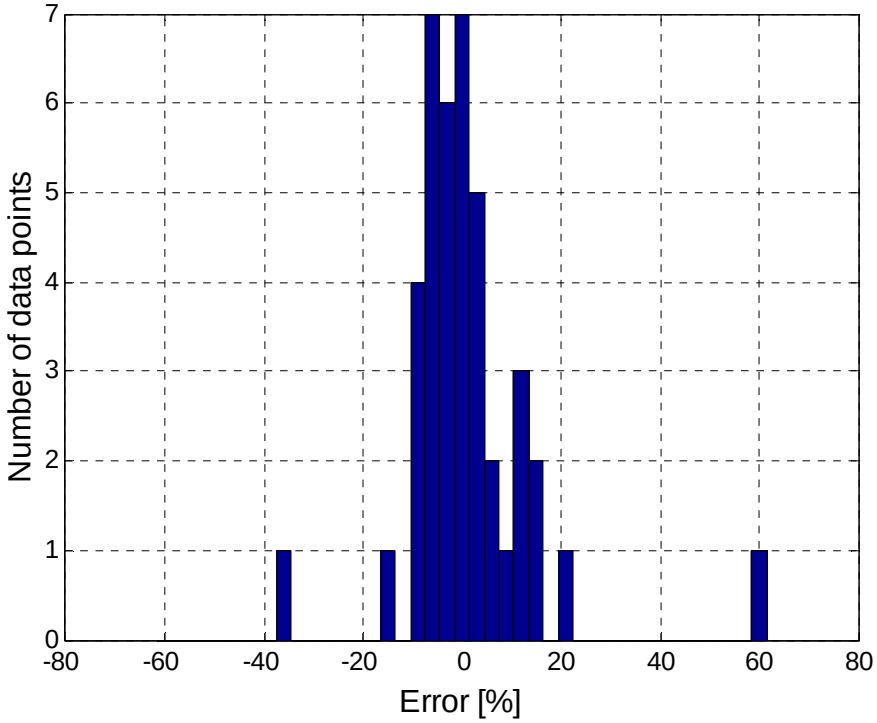

Figure 5.6 Errors using equations (3.1), (3.2), and (4.4).

Using equations (3.1), (3.2) and the look-up table (3.3) the mass flow was modelled, see figures 5.7 and 5.8.

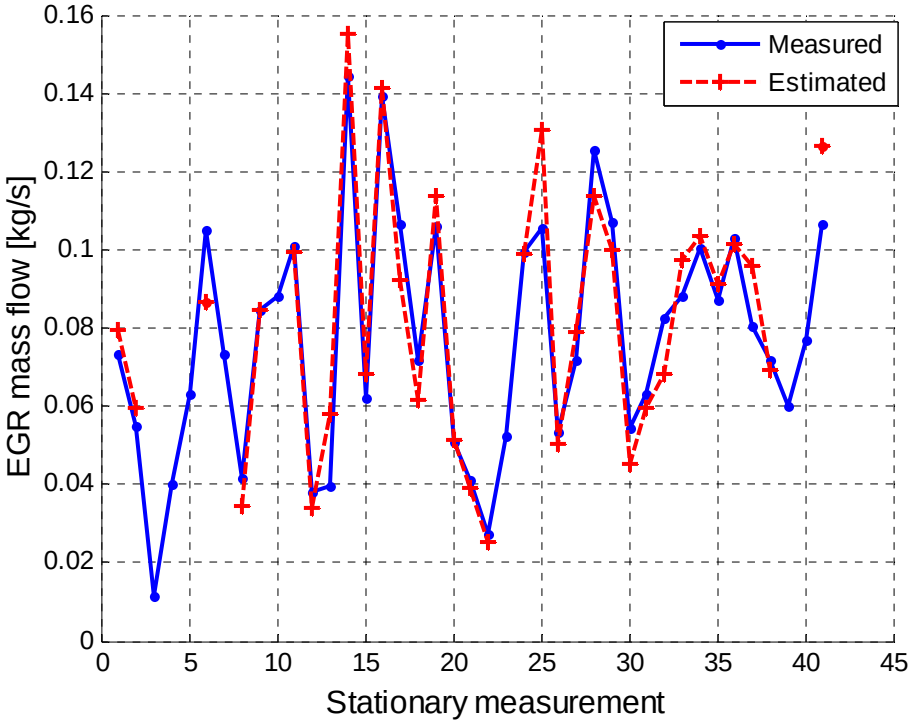

Figure 5.7 Mass flow estimation using equations (3.1), (3.2), and (3.3).

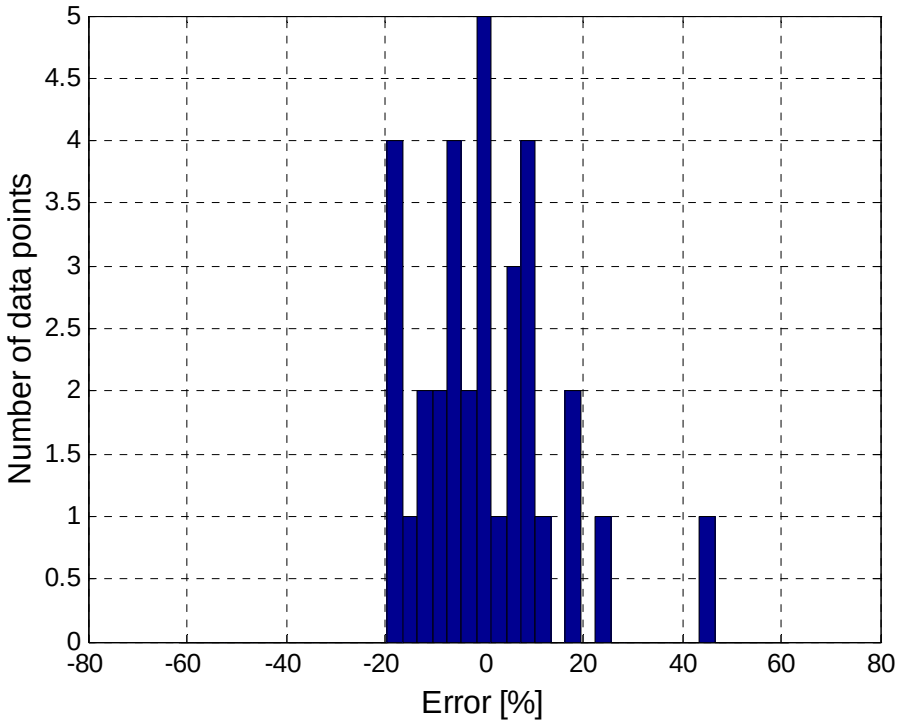

Figure 5.8 Errors using equation (3.1), (3.2), and (3.3).

Taking no notice of the least-squares estimated variables above, look-up table (3.4) was used in combination with equation (3.1) and (3.2). Equation (3.2) was identified with the third data set. The second data set was used for identification of (3.4) and a different part of the second data set was also used for validation. The result can be seen in figures 5.9 and 5.10.

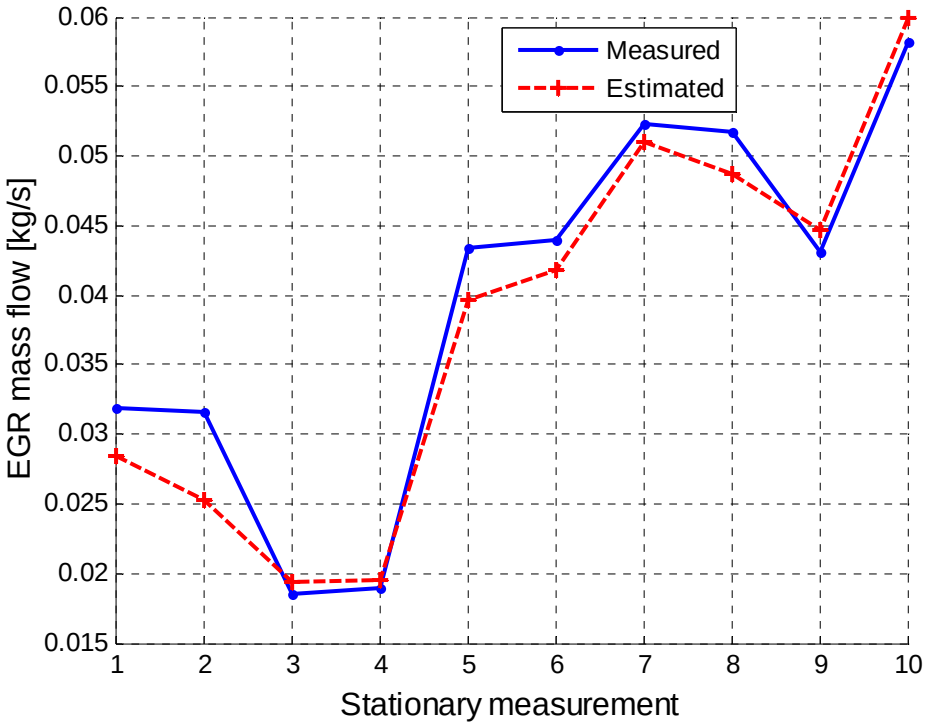

Figure 5.9 Mass flow estimation using equations (3.1), (3.2), and (3.4).

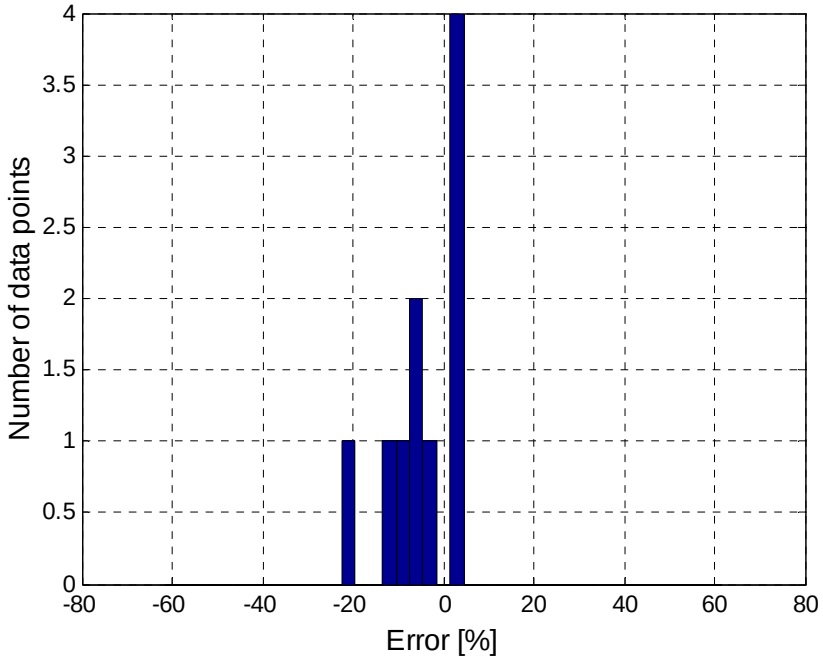

Figure 5.10 Errors using equations (3.1), (3.2), and (3.4).

Even though the second data set did not consist of many data points it was the only data set containing the venturi estimation that was supposed to be surpassed. Validation was therefore performed using the second data set and the aforementioned four models except look-up table (3.4). The validation result can be seen in figure 5.10.

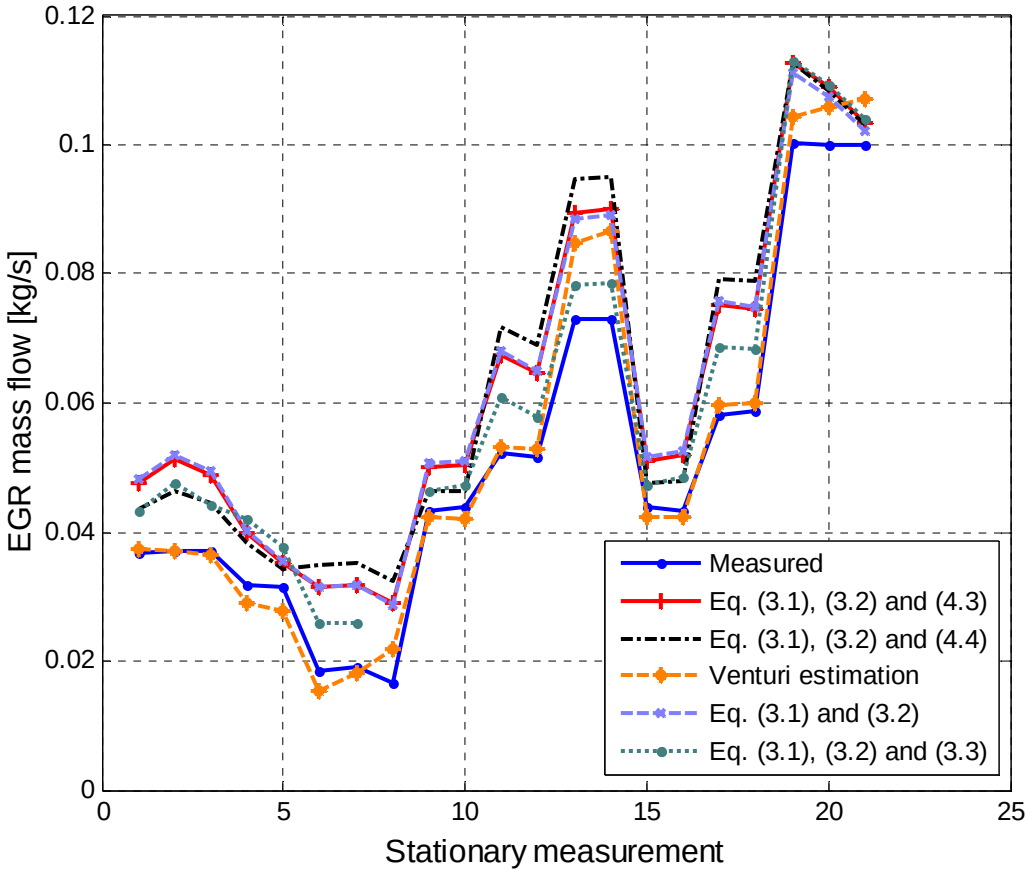

Figure 5.11 Validation of mass flow estimation using the second data set.

To be able to perform some kind of dynamic validation, the delayed CO_2 measurements were compensated for. The signals were moving average filtered and used in the respective models. Equations (3.1), (3.2), and the two versions of (3.5) were tested dynamically, see figures 5.12 and 5.13.

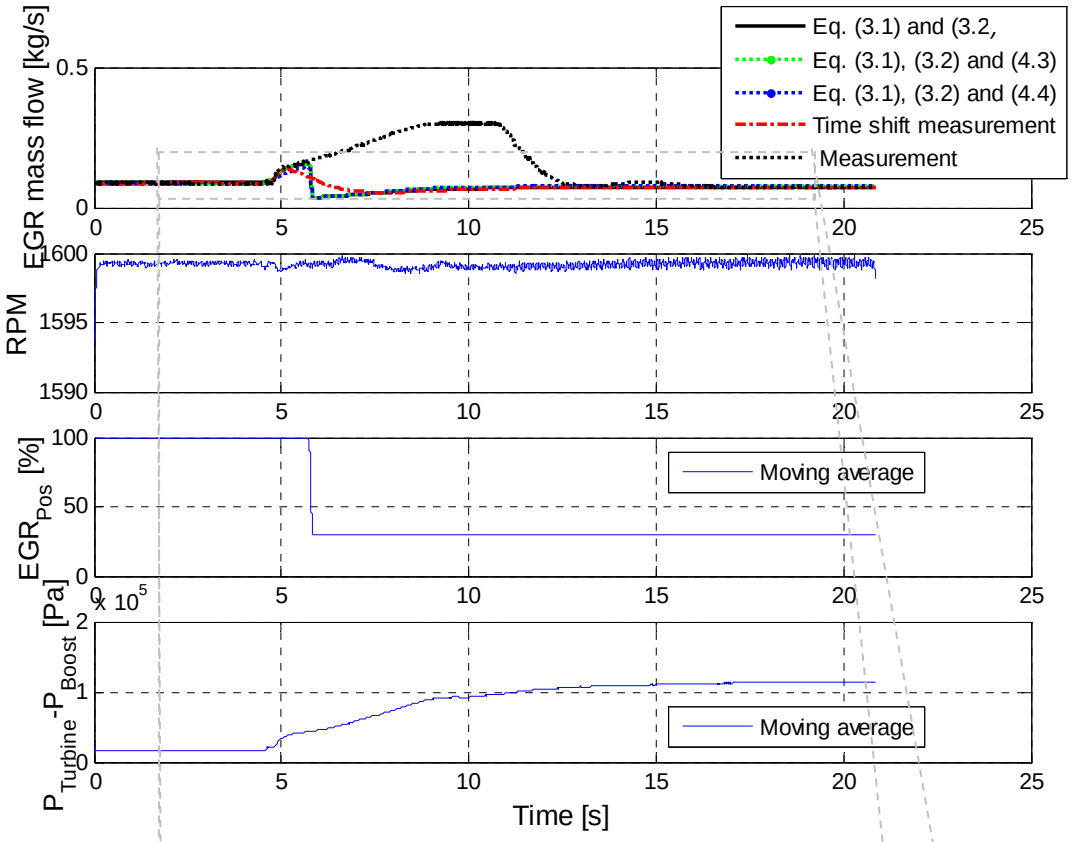

Figure 5.12 Dynamic validation of models.

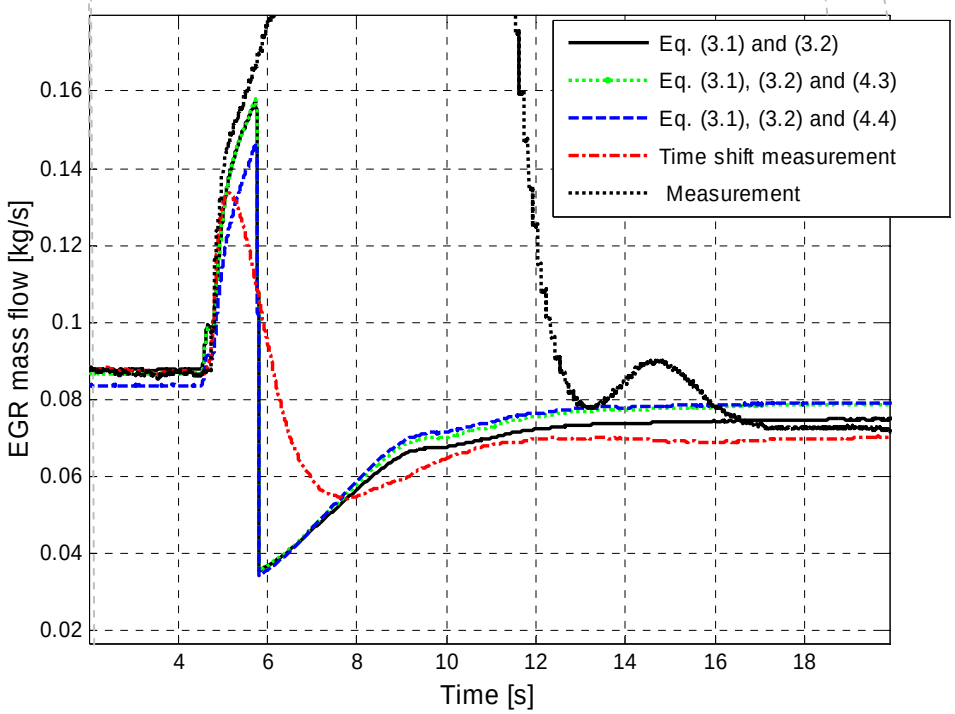

Figure 5.13 Enhancement of figure 5.11.

Since only a few data points were available for identification and validation in the second data set, conclusions regarding equation (3.7) used on the venturi restriction were drawn from the identification data, as seen in figure 5.14 and the errors in table 5.5. Note that a few imaginary flows have been removed. These are the results of a poorly modelled H_{Res} that becomes negative under certain conditions.

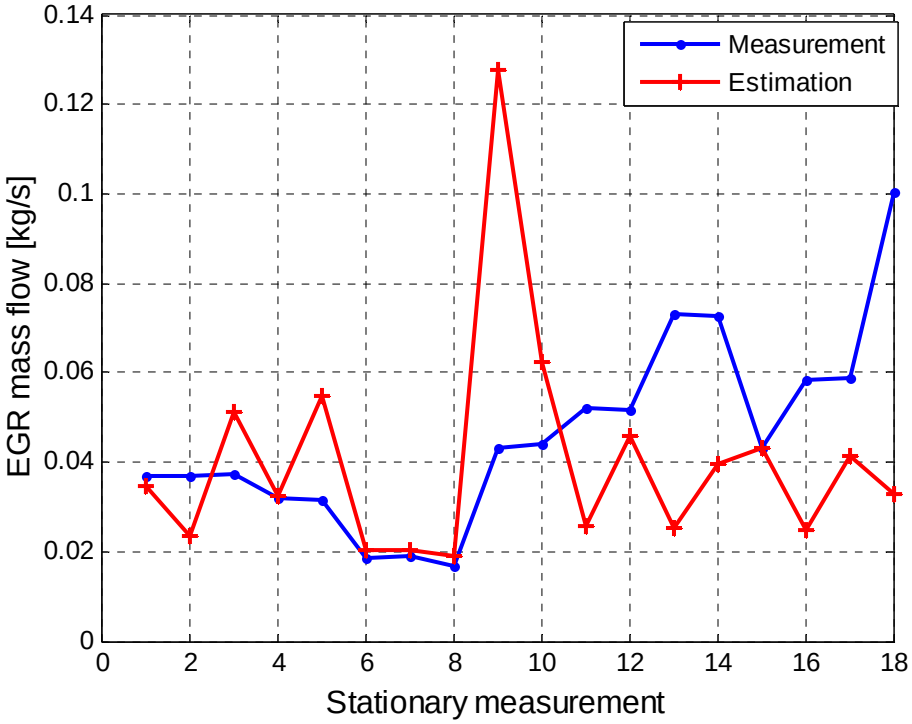

Figure 5.14 Measured and modelled mass flow using equation (3.7) and venturi restriction.

The variance accounted for values from figure 5.12 are as follows

Table 5.1 VAF for the estimations in figure 5.11.

	Equations (3.1), (3.2), and (4.4)	Equations (3.1), (3.2), and (4.3)	Equations (3.1) and (3.2)
VAF (%)	97.07	97.11	97.60

Errors for the models above in stationary validation are presented in tables 5.2 and 5.3.

Table 5.2 Errors for the models using a part of the third data set as validation data.

	Equations (3.1) and (3.2)	Equations (3.1), (3.2), and (4.4)	Equations (3.1), (3.2), and (4.3)	Equations (3.1), (3.2) and (3.3)
Maximum relative error (%)	72.79	59.99	70.03	45.99
Mean relative error (%)	9.42	7.937	9.12	10.07

Table 5.3 Errors for the validated models using the second data set as validation data

	Equations (3.1) and (3.2)	Equations (3.1), (3.2), and (4.4)	Equations (3.1), (3.2), and (4.3)	Equations (3.1), (3.2), and (3.3)	Venturi estimation
Maximum relative error (%)	73.38	95.33	73.92	39	32.45
Mean relative error (%)	28.77	29.45	28.30	16.48	7.19

Table 5.4 describes validation of look-up table (3.4) with data from the second data set that is different from the identification data.

Table 5.4 Validation of look-up table (3.4) with only ten data points from the second data set.

	Equations (3.1), (3.2), and (3.4)	Venturi estimation
Maximum relative error (%)	19.95	16.56
Mean relative error (%)	6.60	5.76

Errors for the incompressible flow model (3.7) used on the venturi restriction are seen in table 5.5. Equation (3.7) was validated with identification data from the second data set.

Table 5.5 Errors for incompressible model estimate, equation (3.7), as seen in figure 5.14.

	Incomp. model estimate eq. (3.7)
Maximum relative error (%)	194
Mean relative error (%)	41.6

5.2 Venturi mass flow error model validation

This subchapter will be excluded and presented in an appendix reserved for Volvo due to Volvo internal policy.

Chapter 6

Concluding remarks

6.1 Sources of error

The EGR cooler will be subjected to fouling which will deteriorate its cooling ability. Also this soot may deteriorate the flow through the EGR channel hence making the mass flow model erroneous. The EGR valve dynamics are not included in the model and only the desired value of the EGR valve position is used. This can worsen errors during dynamic simulation. Furthermore heat losses in changing ambient temperatures may have an effect on the model. For dynamic measurements the delay in rig reference measurements was compensated for by hand and this compensation will therefore be subjected to an error. $P_{TurbineAmplitude}$ showed variations during assessment of this amplitude and an exact value was therefore not attainable.

6.2 Discussion

The impact of CO_2 time shift is very obvious in figure 5.12. The original mass flow measurement has a possible saturation between 8-11 seconds. The time shifted measurement shows the mass flow based on time shifted CO_2 signals. The latter is much more likely even though the pressure difference is increasing. This statement is based on the sudden closure of the EGR valve, which in turn is the result of a load step. The closure will result in a sudden mass flow reduction. It is interesting that the time shifted measurement responds to an EGR valve closure before the latter has even occurred. This is probably the result of an inaccurate assessment of the CO_2 signal delay.

The model errors depicted with histograms generally reveal slight systematic errors. The histogram in figure 5.8 however shows a severe model error rendering this look-up table inadequate. Note that this look-up table, that is (3.3), is not subjected to the same data points from the third data set due to limitations in the look-up table and the data points that risk generating high maximum relative errors are not present in this validation. Using the turbine pressure amplitude to estimate EGR mass flow is a promising way of modelling, as can be seen in figure 5.9. This conclusion is however based on too few data points in the aforementioned figure. To conclude which model, out of equations (3.1), (3.2), and (3.5), that was the best is impossible in dynamic validation using the third data set. Equation (4.4) seems good though in stationary validation using the same set. Validating models identified with the third data set using only the second data set was a disappointment, as can be seen in figure 5.11. It is almost as if there is a constant difference in mass flow between model and measurement. The origin of this offset is unknown.

Modelling the EGR mass flow according to equation (3.6) and (3.7) proved difficult. The reason was that these equations were derived for a constant restriction and they were therefore applied to contant restrictions in the EGR channel, that is venturi and EGR cooler. Neither of these restrictions proved appropriate. The aforementioned equations are only valid for constant energy systems since they were derived from Bernoulli's equation, see equation (6.1). The EGR cooler itself is a severe violation of this principle since there is a difference of a few hundred degrees celsius across the EGR cooler.

$$\frac{\rho \cdot v_1^2}{2} + p_1 = \frac{\rho \cdot v_2^2}{2} + p_2 = \text{constant} \quad (6.1)$$

where indices 1 and 2 signify either side of the restriction. The terms on the respective sides are denoted dynamic and stationary pressures. Assuming that the energy in the system is constant an increase in flow speed will result in a lowered stationary pressure and vice versa. By using the downstream pressure and the known areas of the piping surrounding the EGR cooler the upstream pressure was calculated. This calculated value exceeded that of the upstream pressure measurement and it was therefore concluded that the EGR cooler was a grave violation of the Bernoulli equation validity. It seems as if the theoretical pressure drop is decreased due to the cooling in the EGR cooler.

Using equations (3.6) and (3.7) the venturi was used as a restriction. This choice of restriction and pressures after the EGR cooler should make Bernoulli's equation valid. But this mass flow model also did not surpass the venturi estimation when using only identification data. One reason may have been that the EGR gas mixes with air in the inlet and it is uncertain how this affects the intake pressure. It is however noteworthy that the inlet pressure works much better in equation (3.1). Furthermore an incompressible flow model may be inappropriate simply because the flow is compressible. After all equation (3.1), which works pleasingly, is a compressible flow model.

On condition that a simple equation as the ideal gas law is valid under the exhaust manifold conditions a linear static relationship between pressure and temperature should be valid. This was not the case since the filtered pressure signal was almost sine-shaped which would have required a sine-shaped temperature if the assumption of a stationary linear relation should be valid. If there was a linear transfer function that related the two signals the sine shaped signal should result in a second sine shaped signal with different amplitude and phase but this is also not the case. The nonlinear behaviour might be caused by the slow temperature sensor or it could be assumed that there is no linear relationship between pressure and temperature under these conditions. The coherence plot in figure 4.5 confirms that there is no linear response between T_{Cyl5} and $P_{Turbine}$.

Assessing appropriate placing of pressure sensors was difficult since only a limited number of placements were available. The $P_{EGRCoolerBefore}$ pressure sensor was found to be inappropriate for mass flow estimation with equation (3.1). This may be caused by turbulence or by to small a pressure difference over the EGR valve. The $P_{Turbine}$-$P_{EGRCoolerAfter}$ combination had the smallest maximum relative error. The second data set was however not converted rightly until too late in the work process and the results were therefore not used in the modelling. The difference in errors between $P_{Turbine}$-$P_{EGRCoolerAfter}$ and $P_{Turbine}$-P_{Boost} is nevertheless small. Furthermore the pressure reduction across the EGR cooler was too low in order to constitute the basis for mass flow estimation using equation (3.1) and therefore the pressure downstream, $P_{EGRCoolerAfter}$, sometimes came close to that upstream, $P_{EGRCoolerBefore}$. A mass flow model over the EGR cooler according to equation (3.1) would not have involved the EGR valve position, but since the EGR valve ultimately changes the pressure in the EGR channel its effect may have been taken into account anyway.

Assessing what is a fitting sampling interval will likely depend on the situation. The plot in figure 4.7 is the result of the mean calculation being done in stationarity. The result during transients would be very different. Figure 4.7 never shows an error in P_{Boost} that exceeds 3.5

kPa but the imaginary flow occurs already at 1.5 kPa. 1.5 kPa or below seems to require faster sampling than every 100^{th} data point. On the other hand a mass flow error of maximum 10 % in figure 4.7 would require faster sampling than every 50^{th} data point, according to figures 4.6 e) and f). Figure 4.7 suggests a faster sampling than every 40^{th} data point if the ± 10 % error limit should be fulfilled. Note that imaginary flow occurs when only every 120^{th} data point is included in the mean calculation in figure 4.8.

6.3 Conclusion

Mean value models of the EGR mass flow in a Volvo diesel engine have been developed. Validation indicates that they are not improvements on the existing venturi mass flow estimation. The validation should be trustworthy. Equations (3.1), (3.2), (4.3) and (4.4) offer models whose performances can hardly be distinguished from one another in dynamic validation but show great differences when subjected to the second data set. Equation (4.4) excels when only validating with the third data set. Look-up table (3.3) is probably not an improvement on (3.2). Look-up table (3.4) seems to work well but the amount of identification and validation data is somewhat lacking. There is no linear connection between $P_{TurbineAmplitude}$ and EGR mass flow.

It seems inappropriate to sample slower than every 40 crank angle degrees.

The combination $P_{Turbine}$ and $P_{EGRCoolerAfter}$ showed the smallest maximum relative error and this was the best pressure combination for use in the mean value models.

Assessing the way cylinders burn can not be done with the existing sensors, only.

6.4 Future work

Equation (3.7) can probably be developed further, maybe by using a look-up table. Nonlinear identification of temperature and pressure or identification of a connection between exhaust manifold pressure and the temperature in the respective cylinders can probably be performed. A first step may however be the use of fast temperature sensors. The assessment of good pressure sensor placing might include coherence between pressures and mass flow.

References

[Eri04] C. Ericson. *Mean value modelling of poppet valve EGR-system*. Master thesis LiTH-ISY-EX-3543-2004, Department of electrical engineering, Linköping University, Linköping, Sweden, June 2004

[Gla91] T. Glad and L. Ljung. *Modellbygge och simulering*. Studentlitteratur, Lund, 1991

[Hen99] E. Hendricks. *Mean value modelling of an SI engine with EGR*. SAE international, Warrendale, PA, USA, 1999

[Hey88] J. Heywood. *Internal combustion engine fundamentals*. McGraw-Hill book company, 1988.

[Höc06] E. Höckerdal and A. Jerhammar. *Gas flow observer for a Scania diesel engine with VGT and EGR*. LiTH-ISY-EX—06/3807--SE, Vehicular systems, Linköping University, Linköping, Sweden, February 2004

[Joh06] R. Johansson. *System modeling & identification*. Dept. Automatic Control, Lund University, Lund, 2006.